INFRARED SPECTROSCOPY IN CLAY SCIENCE

PAUL A. SCHROEDER

CONTENTS

Schroeder, P.A. (2002) Infrared Spectroscopy in clay science: In CMS Workshop Lectures, Vol. 11, *Teaching Clay Science*, A. Rule and S. Guggenheim, eds., The Clay Mineral Society, Aurora, CO, 181-206.

INFRARED SPECTROSCOPY IN CLAY SCIENCE

PAUL A. SCHROEDER

Department of Geology
University of Georgia
Athens, GA 30602-2501 USA

INTRODUCTION

Infrared (IR) spectroscopy is a common technique with spectrometers capable of good-quality mid-IR absorption data (i.e., in the 400 to 4000 cm^{-1} range) available in most undergraduate chemistry teaching laboratories. Sample preparation is relatively simple and requires only KBr powder, a die press, and a balance. An understanding of the interaction between electromagnetic radiation and crystalline material is required to comprehend IR absorption phenomenon (and other vibrational spectroscopies). Also required, is a description of symmetry elements within molecular clusters and crystalline compounds.

Examination of the mid-IR absorption spectra and an explanation of the structural models of the minerals brucite, gibbsite, kaolinite (kaolin group), lizardite (serpentine group), talc, pyrophyllite, and clinochlore (chlorite group) provide a basis for understanding most of the constituent units of clay minerals. These units include the hydroxyl groups, tetrahedral silicate/aluminate anions, octahedral metal cations, and interlayer cations. O-H stretching modes common to most phyllosilicates lie in the spectral region of 3400 to 3750 cm^{-1}. Metal-O-H bending modes occur in the 600 to 950 cm^{-1} region. Si-O and Al-O stretching modes are found in the 700 to 1200 cm^{-1} range. Si-O and Al-O bending modes dominate the 150 to 600 cm^{-1} region.

Lattice vibrational modes in the far-IR range (33 to 333 cm^{-1}) are related to the interlayer cation. The study of mid- and near-IR modes using reflectance techniques and spectrometers with environmental controls require specialized equipment. This instrumentation is becoming more common. Thus, IR spectroscopy allows students to better understand the structural components of clay minerals and how these components respond to changing environmental conditions.

The purpose of this chapter is to (1) introduce the principals of vibrational spectroscopy and (2) familiarize teachers and students with IR spectra of well-characterized minerals whose features can identify structural groups within clay minerals.

BACKGROUND

Structures

The structures of clay minerals are often depicted as ball-and-stick models. With such models, it is easy to envision the arrangement of oxygen and metal atoms into symmetric tetrahedral (four nearest-neighbors) or octahedral (six nearest-neighbors) coordination schemes (Fig. 1). Models improve our

understanding of clay-mineral atomic structure, which in turn helps us to predict the physical and chemical behavior of clay minerals. However, the atoms found in clay minerals are not fixed in space like the desktop models we hold in our hands. Atoms are electrically charged entities that vibrate at frequencies in the range of 10^{12} to 10^{14} Hz and, in some cases, they can move from one to another structural site to within the crystal.

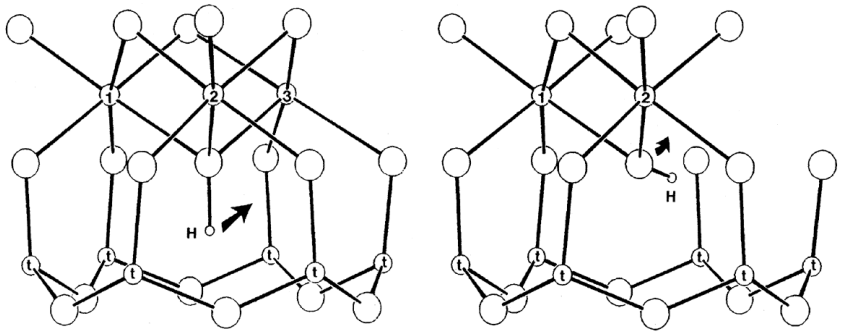

Figure 1. Schematic diagram of trioctahedral (left) and dioctahedral (right) layer structures common to all clay minerals. Octahedral sites (1, 2, and 3), tetrahedral sites (t) and protons (H) are depicted in coordination with oxygen. Left arrow indicates the reorientation of O-H that occurs upon heating and oxidation of Fe in clay structures. Right arrow indicates the relocation of O after heating-induced dehydroxylation. (Figure from Schroeder, 1990).

Theory

The theory of crystal vibrations is extremely complex. Spectra that can be interpreted on first principles are a rarity. The interpretation of spectra and their relationship to clay-mineral composition and structure is, in part, accomplished by comparing families of mineral spectra and correlating those spectra with other measures of crystal chemistry. Molecular-orbital theory calculations for interpreting vibrational spectra (Kubicki, 2001) will soon be available to clarify spectral interpretations. Those interested in the theoretical treatment of crystal vibrations can begin by consulting Farmer (1974). This chapter is limited to the comparison of empirical relationships. A simplified treatment is presented below with references for those who are interested in learning more about vibrational spectroscopy.

Oscillating electric and magnetic fields of electromagnetic (EM) radiation can interact with the atoms in different ways, one of which is the absorption and scattering of light energy (Fig. 2). The study of the interaction between infrared (IR) electromagnetic radiation and the vibrational motion of atomic clusters constitutes part of the field of vibrational spectroscopy. Electronic spectroscopy involves the interaction of visible and ultraviolet EM radiation and electron transitions. The study of IR absorption is known as IR spectroscopy. The study of light scattering is Raman spectroscopy. In this chapter, the focus is on the infrared portion of the EM spectrum and the absorption phenomenon. The field of IR spectroscopy has an extensive record of successful applications in nearly every branch of science. For those interested in

the subject, there are more advanced introductions to symmetry and spectroscopy (e.g., Harris and Bertolucci, 1978; Calas and Hawthorne, 1988; McMillan and Hess, 1988). The intent herein is to provide a minimal theoretical background, such that students can visualize the IR absorption phenomenon and factors that influence IR spectral response.

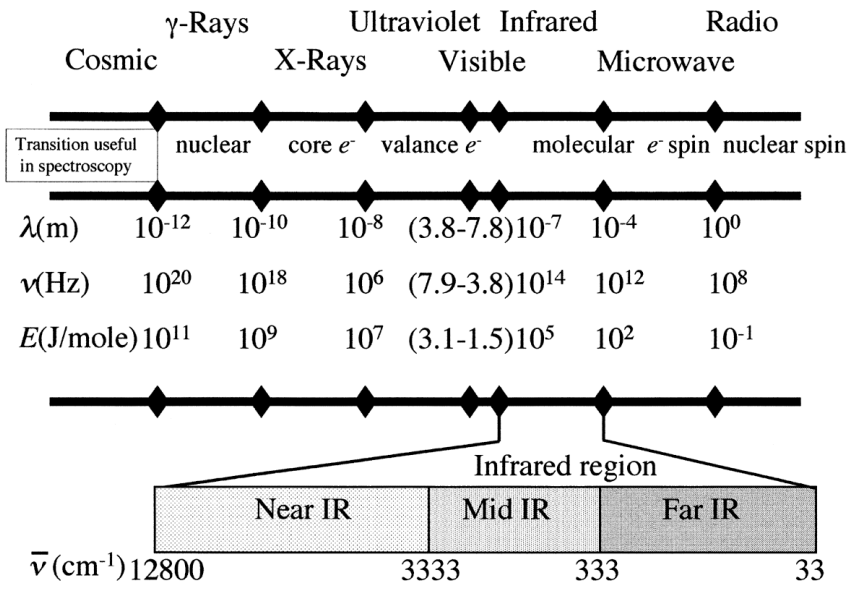

Figure 2. The electromagnetic spectrum. λ is wavelength in meters, Hz is frequency in cycles per second, and *E* is the energy associated with a mole of photons, in joules. Values tabulated are in order of magnitude (except the boundaries for visible light, which are common reference points). Also included are transitions responsible for absorption phenomena that are employed in spectroscopy.

One prerequisite for EM radiation absorption is that a "resonance match" occurs between the vibrational energy of the bonds in clay minerals and the energy of EM radiation (Fig. 2). In other words, IR radiation excites vibrations of the same frequency. The energy match produces an absorption phenomenon that involves an energy change or transition. The difference in energy (ΔE) for the transition is related to the frequency of radiation (υ) by Planck's constant (h).

$$\Delta E = h\upsilon \tag{1}$$

As the frequency of electromagnetic radiation is related to the velocity of light in a vacuum (c) and the wavelength of the radiation (λ),

$$\upsilon = \frac{c}{\lambda} \tag{2}$$

then,

$$\Delta E = h\frac{c}{\lambda} \quad (3)$$

Thus, as the energy of a transition increases, the corresponding frequency increases, and the corresponding wavelength becomes shorter.

Many units are used in vibrational spectroscopy (which can be confusing to both experts and non-experts). The unit of wavenumber (cm^{-1}) is more commonly used in IR and Raman spectroscopy. In general, the frequency range of 10^{12} to 10^{14} Hz roughly translates to the IR ranges of 33 – 12,800 wavenumber (cm^{-1}) or 0.4 - 150 kJ mol^{-1}. The IR frequency range is further subdivided into the near-IR (12,800 to 3333 cm^{-1}), mid-IR (3333 – 333 cm^{-1}), and far-IR regions (333 – 33 cm^{-1}) for convenience of discussion.

Molecular and crystal vibrations

Two or more vibrating masses connected by springs is a simple analogy to envision molecular clusters. As each atom in the clay structure is displaced relative to each other, a complex set of motions occurs. Their relative magnitude and sense of movement in a normal coordinate system describe these motions. These motions are qualitatively characterized as symmetrical and asymmetrical stretches, bends and rocking. Understanding symmetry is key to understanding the energy levels in a crystal.

Exploration Phase Activity 1. Ask students to name factors that influence the modes of vibration a crystal exhibits when irradiated with infrared radiation.

Vibrating atoms in a crystal structure exhibit a complex set of motions. These motions are intimately related to the symmetry of the crystal structure. Energy levels of different crystal structure symmetries can be modeled by considering the potential energy of three blocks of different geometry resting alternately on each of six faces. Ask students to work in small groups. Give each group three blocks of equal mass: a cube, a stretched cube (square prism) and a shoebox or brick-shaped block (rectangular prism). Ask students to determine the number and relative magnitudes of different potential energy levels for each block by placing each block alternately on each of its six faces and gauging the ease or difficulty of pushing the block over. Ask students to present their findings as a chart that lists the different potential energy levels for each block. Then ask students to explain how symmetry might affect the number of vibrational modes of atoms in a crystal.

One easy way to view the relationship between symmetry and energy levels is to examine three blocks of equal mass whose sides have lengths where $a = b = c$ (cube); $a = b < c$ (stretched cube); and $a < b < c$ (shoe box). Each block has six possible stable resting positions (Fig. 3). The potential energy for each block depends upon the face that is down.

The potential energy (*PE*) is calculated by knowing the mass (m) of the block, the acceleration of gravity (g) and the height (h) of the center of mass above the surface upon which the block rests (i.e., the resting face). The

symmetry elements of the blocks are such that we can divide them into three groups depending upon the resting face. The cube has identical energy potential regardless of the resting face. This is referred to as degeneracy (the number of states with exactly the same energy level). The cube can be considered triply degenerate. The stretched cube has two possible energy states. The potential energy is the greatest when resting upon the *ab* face. Resting on the *ac* and *bc* faces results in a doubly degenerate state. The shoebox-shaped block has three potential energy states. The energy diagram shown in Figure 3 is analogous to energy states for molecules and crystals. The more symmetric the structure, the fewer different energy levels it has, and the greater the degeneracy.

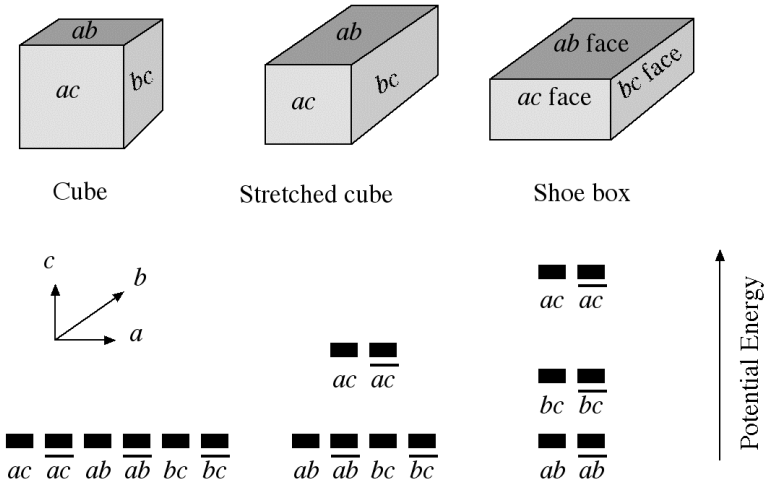

Figure 3. Potential-energy analogy for symmetry energy states in a crystal. The mass of each parallelepiped (block) is assumed equal. The higher the center of mass, the greater the energy. Although an infinite number of energy states are possible, resting on one of six faces represents the most stable potential energy states for each block. The bars at the same height below represent each resting position having a degenerate energy level. For example, the cube has six energy states at the lowest level.

Exploration Phase Activity 2. Consider the H_2O molecule. The oxygen and hydrogen atoms are represented as point masses and the attractive and repulsive forces of bonding are represented by springs whose displacement is defined by a force constant (*e.g.*, Hooke's law). An isolated H_2O molecule is characterized by the geometric arrangement where the average O-H distance is 0.957 Å and the average H-O-H angle is 104.5°. The relative motions of the vibrating H_2O molecule correspond to a pattern of normal modes that move with specific vibrational frequencies. Suppose that infrared light, which has a frequency range of 9.9×10^{11} Hz to 3.8×10^{14} Hz, is passed through water vapor. The ground state of the molecule energy is promoted to its first excited vibrational state. The

H_2O molecules can vibrate in different ways. Ask students to determine the possible vibrational modes of an H_2O molecule by drawing arrows indicating relative motions of atoms on Figure 4. Arrows on hydrogen atoms should indicate motion in directions parallel or perpendicular to the individual bonds with oxygen, whereas arrows on the oxygen atom should indicate motion parallel or perpendicular to the plane of hydrogen bonding. Figure 5 is a reproduction of Figure 4 with the arrows correctly placed.

In the case for the three atoms in an H_2O molecule, there are three normal modes of vibration (Fig. 5). The first mode is a symmetrical stretching mode that ideally vibrates at 1.095×10^{14} Hz. This translates to a transition energy of 43.7 kJ mol^{-1} which may also be manifested as a spectral absorption band at 3652 cm^{-1} in the IR spectrum (if absorption occurs). A second bending mode occurs at 1595 cm^{-1} and a third asymmetric mode occurs at 3756 cm^{-1}. Although all three of these vibrational modes are present in the H_2O molecule, the extent of IR absorption that occurs depends on the symmetry of the vibrational motion.

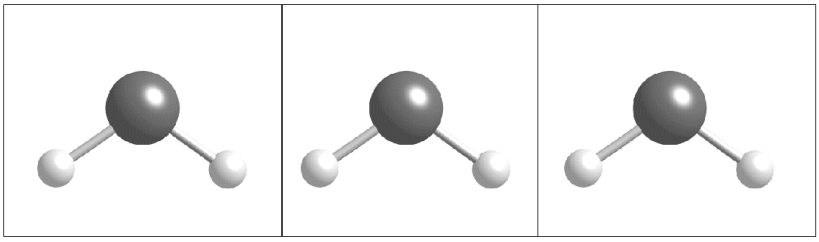

Figure 4. The normal modes of vibration for water. Small atoms are protons. Determine the possible vibrational modes of the H_2O molecule by drawing arrows indicating relative motions of atoms. Arrows on hydrogen atoms should indicate motion in directions parallel or perpendicular to the individual bonds with oxygen, whereas arrows on the oxygen atom should indicate motion parallel or perpendicular to the plane of hydrogen bonding.

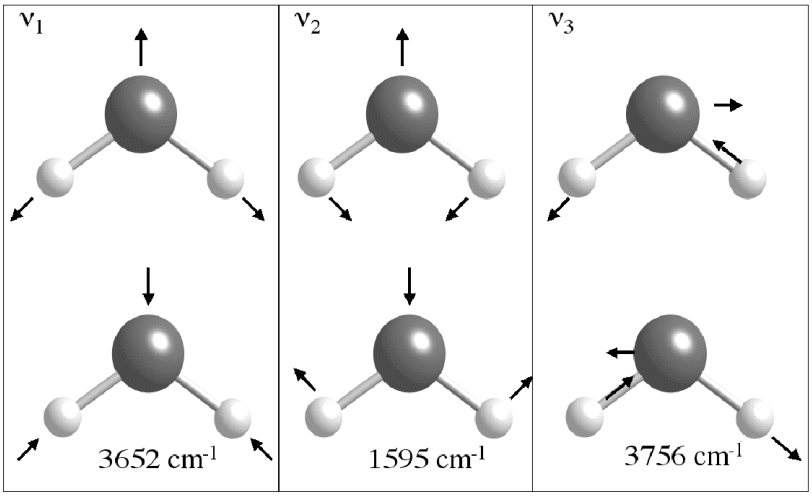

Figure 5. The three normal modes of vibration for water. Small atoms are protons. Arrows represent directions of motion of each atom when the molecule vibrates. The reciprocal motion is shown for each mode. Note that the change in normal mode ν_3 motion can be described by a symmetry operation that involves a 180° rotation (C_2) about a vertical axis through the oxygen atom.

The number of fundamental normal modes in a molecule is equal to 3N-6, where N is the number of atoms in the cluster or unit cell. The six that are subtracted include three rotational modes and three translational modes. For example, H_2O has three fundamental modes (i.e., (3 x 3) – 6 = 3, where, ν_1= 3652 cm^{-1}, ν_2= 1595 cm^{-1}, and ν_3= 3756 cm^{-1}).

Clay minerals are different from H_2O molecules in that their atoms are arrayed into a periodic crystalline structure. The influence of the vibrational motion of nearing neighbors arranged into a lattice pattern results in displacement waves that travel through the crystal. These waves are known as lattice vibrations. If nuclear displacements are parallel to the wave propagation, then the lattice waves are called "longitudinal" and when displacements are perpendicular, then they are called "transverse". Clay minerals can contain a large number of atoms per unit cell. If for example, N = 50, then the number of fundamental modes equals 147 (only three are subtracted because the unit cells can not rotate). Fortunately not all fundamental modes are IR active and therefore, not every mode appears as an absorption band in a spectrum. Not all modes are IR active because the electric field induced by the incident radiation must interact with the change in dipole moment associated with a specific vibrational mode. The dipole moment is simply a function of the magnitude of the charge of two particles and the distance between them. Not all vibrational modes interact with an electric field of light, and they do not have the same intensity of absorption. The extent of absorption is governed by "selection rules". Selection rules are based on the approximation of a harmonic oscillator (i.e., Hooke's law version of charged atoms connected by springs). A vibrational

transition is IR active if the dipole moment of the molecule changes during the vibration. The oscillating dipole absorbs energy from an oscillating electric field if, and only if, they oscillate at the same frequency.

A good analogy is to recall the ease of pushing a child on a swing at the same frequency that the child is pumping. It is difficult to push at a frequency that is out of phase with the child. The "push" in vibrational spectroscopy occurs when the negative charge on the molecule is in phase with the negative sign of the electric field. If the light frequency and the vibrations are not the same, then the energy transfer does not occur.

In typical IR experiments, the frequency of EM radiation ranges from 2000 to 20 cm^{-1} (i.e., the wavelength ranges from 5 x 10^4 to 5 x 10^6 nm). This is much larger than the unit cell dimensions of clay minerals, which typically range from 1 to 10 nm (10 to 100 Å). Consequently, only very long wavelength lattice vibrations can interact with light in an IR experiment. These vibrations are called the "optic modes". Transverse and longitudinal optic modes are termed *TO* and *LO* modes.

As an aside, if a dipole moment is induced by placing a molecule in an electric field, then the extent to which the dipole can be changed is called "polarizability". In this case, a transition or vibrational mode is Raman active if the polarizability of the molecule changes during the vibration. However, not all modes will be IR and/or Raman active. The focus of this chapter is IR absorption, but the two forms of IR and Raman spectroscopy are complimentary and a full understanding of clay-mineral properties can only be obtained using the collective study of the IR, Raman, and other spectroscopies, as well as such methods as X-ray and electron diffraction.

In addition to fundamental modes, just as in musical tones, overtones and combination modes can form. Overtone and combination modes are additive and typically occur in the higher frequency near-IR region. Overtones and combination modes can be calculated from theory by the position of fundamental modes in the mid-IR region (*i.e.*, overtones = $2\nu_1$, $2\nu_2$, $2\nu_3$ and combinations = $\nu_1+\nu_2$, $\nu_2+\nu_2$, $\nu_1+\nu_3$). Overtones and combination modes are useful in clay science, because they often help to distinguish between adsorbed H_2O, structural H_2O, and structural hydroxyl (OH) groups. Overlap of fundamental vibration modes in the mid-IR range often makes it difficult to distinguish the various forms of H_2O. This is where combination and overtone modes are helpful. Madajová and Komadel (2001) provide several examples of near-IR spectra and the occurrence of overtones and combinations modes in clay minerals.

In general, the following relationships can be applied to the IR spectroscopic investigation of clay minerals based on the principles of selection rules: (1) If the vibration is perfectly centrosymmetric, then the IR mode is not active. However, as in most crystals, the occurrence of nearest neighbor atoms tends to influence the symmetry of atomic coordination. The distortion of symmetry in the crystal and its functional groups therefore determine much about the nature of IR absorption and scattering. (2) Symmetric stretches are usually weaker and lower in frequency than asymmetric stretches. (3) Bending vibrations are lower in frequency than symmetric stretches. (4) Vibrational

modes involving higher valance bonding will be higher in frequency than those involving lower valance bonding (given similar atomic masses and coordination states). (5) Vibrational modes of bonded groups with higher mass will have modes lower in frequency than those of lesser atomic mass (given equivalent valance and coordination states).

Instrumentation and sample preparation for IR experiments

Absorption spectra are obtained by passing an IR beam through a thin film of powdered sample. The KBr-pressed pellet technique is the most commonly used method for preparing solid samples and for collecting spectral data in the mid-IR range. Samples are ground finely in a mortar and pestle. Masses of 0.3 to 2.0 mg are mixed with 150 to 200 mg of IR-grade KBr. The powdered mixture is transferred to a die press that has a typical diameter of 13 mm. The mixture is pressed (~5 kg cm^{-2}) under vacuum to help remove adsorbed H_2O. Under these conditions the KBr anneals into a hard, disc-like pellet that is then placed into a spectrometer for analysis. If samples are not analyzed immediately, then they are placed in an oven at 120° to 150° C to minimize H_2O absorption onto the hydroscopic KBr. Heating to 150° C many times removes molecular H_2O from the mineral surface. However, depending upon the clay type, molecular H_2O may not be removed. Also it is sometimes possible to promote a chemical exchange between the clay and KBr, which might result in a change of the crystalline structure of the clay (Pelletier et al., 1999).

There is a wide array of other experimental apparatus and sample treatment options for the clay science researcher. Some examples include: (1) the ability to collect data in the near-IR and far-IR regions, (2) to make experiments under different environmental conditions (*i.e.,* temperature, pressure, and saturation states), and (3) to utilize reflectance techniques. The advent of Fourier Transform (FT) instruments has increased instrument sensitivity to the point where reflectance techniques, such as attenuated total reflectance (ATR) and diffuse reflectance infrared Fourier Transform (DRIFT) are becoming routine in research laboratories. Sample preparation for ATR and DRIFT techniques may be as simple as placing powdered samples into the devices. ATR and DRIFT attachments will probably become more common in teaching laboratories. There are some differences between absorption and reflectance spectra owing to orientation and scattering effects. However, the data produced from these two methods are equally applicable in teaching clay science. Madajová and Komadel (2001) provide excellent comparisons of transmission and reflectance spectra for clay minerals.

Transmission mode FTIR spectrometers are commonly available in most every undergraduate chemistry laboratory, and it is assumed here that an instrument and sample-preparation equipment are accessible. Access to a teaching-grade FTIR allows students to collect absorption spectra with sufficient quality to illustrate the spectral features shown in this chapter.

FTIR spectrometers are based on a very simple optical device called an interferometer (Fig. 6). Interferometers employ a beamsplitter that takes an incoming infrared beam and divides it into two optical beam paths. The source

of the infrared beam is a heated silicon carbide “globar”. There are several ways to direct the split beam; one approach is to reflect the split beam from a fixed mirror while at the same time reflecting the other portion of the split beam from a moving mirror. The two beams then recombine back at the beam splitter. As the moving beam and fixed beam re-combine, they are redirected by the beam splitter to a detector. The resulting combined wavelengths create a signal known as an “interferogram.” Spitting two beams and reflecting from opposing ends of a rocking mirror can create the same effect as the fixed and moving-mirror combination.

The resulting interferogram now contains unique information about each frequency of EM radiation in the IR spectrum. Thus, all frequencies are measured simultaneously with one pass of the mirror. The interferogram has the frequency information encoded within the time domain (i.e., the reference frame being that of the rate and distance displaced by the moving mirror). Transformation of the time-domain information to the frequency domain is obtained by the Fourier-transform mathematical technique. The rapid speed of data collection allows for the collection of multiple spectra and their subsequent co-addition. Co-addition improves signal-to-background noise approximately according to a square law, where signal-to-noise ratios decrease at a rate equivalent to the square root of the number of scans (e.g., sixteen co-added scans will have twice the signal to noise as four co-added scans).

The end product is an intensity measurement of the IR spectrum. A modern FTIR experiment therefore consists of the following elements: (1) the IR globar source, (2) the interferometer, (3) the sample, (4) a detector, and (5) a computer to perform the FT. The most common detector is a thermal detector made of deuterated triglycine sulfate (DTGS). Heat supplied by the incoming infrared thermal radiation alters the cell dimensions of the crystal, thus changing the value of the electrical polarization. The surface of the crystal perpendicular to its polarization axis can be monitored electronically. Note again, the importance of symmetry. The detector material must be a non-centrosymmetric crystal to exhibit this pyroelectric effect.

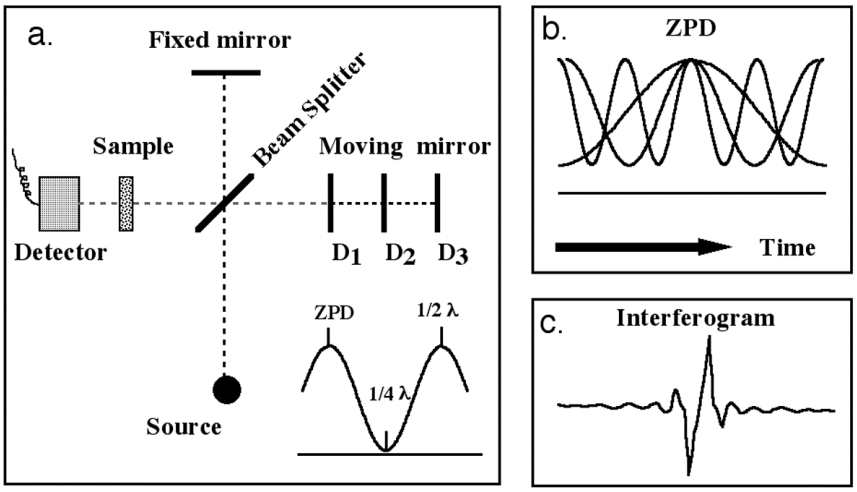

Figure 6. Schematic diagram of a FTIR spectrometer. (a) Dashed lines represent the beam path. D_1, D_2, and D_3 represent displacements of the moving mirror. At the zero point of displacement (ZPD), the path lengths of fixed beam and moving mirror beam are equal and all wavelengths are coherent. (b) As the path length changes, a broad range of IR wavelengths (3 are shown for clarity) are encoded into the time domain. (c) The sum of the signal is an interferogram. This is time domain signal is mathematically converted to a frequency domain spectrum via a Fourier transformation.

Non-linearity of the source intensity, the beam-splitter efficiency, and detector efficiency over the infrared range makes it difficult to absolutely measure absorption spectra. In fact, the absolute intensity in any one experiment is very irregular throughout the IR spectral range recorded. Therefore, an instrument background spectrum is collected. The background may include a blank of the substrate carrier (i.e., a 150 mg KBr pellet). The intensity recording for each frequency of the sample is then divided by the instrument background. The resultant spectrum is recorded as a percent transmittance value (%T = 100 I/I_O), where I is the intensity of sample and I_O is the intensity of the instrument blank at each frequency in the experiment. A transmittance value of 100% is equivalent to complete transparency, whereas a transmittance value of 0% is equivalent to being opaque.

The amount of IR adsorption is related to symmetry of the molecular cluster and the magnitude of the change in the dipole moment. The extent of absorption is also proportional to the amount of material present. IR spectroscopy therefore offers the potential for quantitative analysis based on the Beer-Lambert Law. The Beer-Lambert Law states that in dilute systems, absorbance is proportional to the concentration of absorbing species present:

$$A(\nu) = m(\nu)Ct \tag{4}$$

where A is the absorbance at a measured frequency ν, and defined as $A = -\log(I/I_O)$ or $A = -\log(\%T/100)$. The molar absorptivity (m) of that species is at

frequency ν, C is the concentration, and t is the path length of the IR beam through the sample. It is critical that all factors remain as constant at possible when calibrating for m (see e.g., Schroeder and Ingall, 1994).

RESULTS AND DISCUSSION

Explanation Phase Activity

Provide Figs. 6, 7, 8, 9, 10, 11, and 12 to students who are working in small groups. Ask students to compare and contrast the IR spectra of the different minerals and to suggest reasons for the similarities and differences. Consider such factors as lowering of symmetry by ion substitutions, the presence of interlayer cations, dioctahedral or trioctahedral occupancy of the octahedral sheet, positions of hydroxyl groups, and distortion or rotation of tetrahedra owing to changes in the octahedral sheet. Which of these features occur in the crystal structures of the given minerals? What effect do these factors have on the vibration modes of the crystal structures? Allow groups to share their ideas with the rest of the class, then present the following explanations.

Spectra presented in this chapter were collected using a Bruker Equinox 55 FTIR spectrometer, with a globar source and DTGS detector. Each sample was weighed to within a range of 0.30 to 0.40 mg and mixed with 150 mg of KBr. Each spectrum contains sixteen co-added signals that is divided by a similarly co-added instrument background signal that included a blank 150-mg KBr pellet. Transmittance units were converted to absorbance units and IR spectra are presented as plots of absorbance versus wavenumber. Only some examples are given here; refer to Russell and Fraser (1994) for additional spectra. They present an excellent selection of IR spectra over the range of 4000 to 250 cm^{-1} (in units of transmittance) for clays and associated minerals.

Hydroxide sheets

The octahedral sheet is a basic structural unit common to all clay minerals. IR study of the octahedral sheet configurations can be understood by examination of the hydroxide-group minerals brucite [$Mg(OH)_2$] and gibbsite [$Al(OH)_3$]. Brucite contain sheets where all three octahedral sites ("trioctahedral sheets") are occupied and gibbsite contains sheets with two of three sites ("dioctahedral sheets") are occupied. These sheets are similar to octahedral sheets in phyllosilicates and their study allows for an appreciation of the role of protons in clay minerals.

Figure 7 shows the IR spectrum and atomic structure of brucite. The coordination of Mg^{2+} ions with six nearest oxygen neighbors in the sheet result in an octahedral edge-sharing arrangement. A free OH molecule has six degrees of freedom consisting of a stretching vibration, two rotations, and three translations.

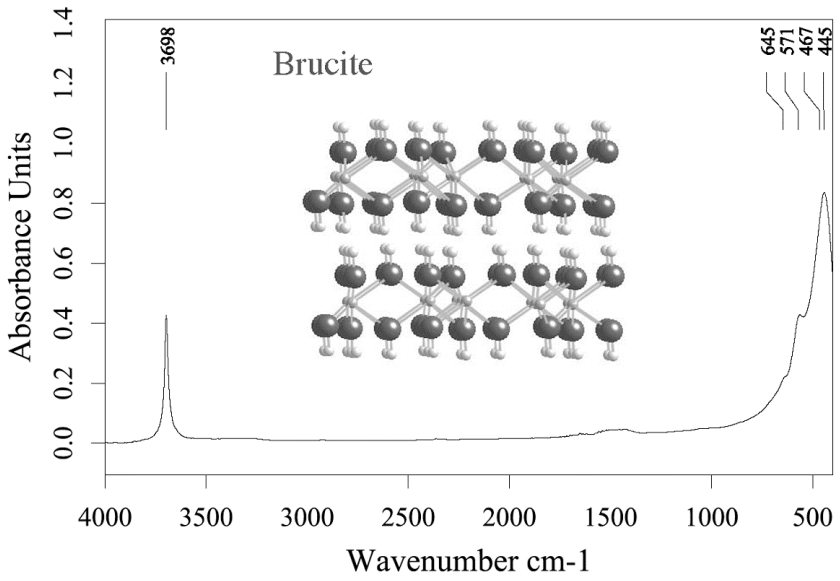

Figure 7. IR spectrum of brucite, $Mg(OH)_2$, using 0.33 mg sample/ 150 mg KBr. Sample from Wood's Chrome Pit, Lancaster County, Texas, PA (Courtesy, James J. Howard). Crystal structure data from Zigan and Rothbauer (1967).

When the OH is bound in the crystal the translations and rotations become vibrations, thus making six vibrations in all. Each OH^- ion in brucite occupies three-fold site symmetry (Ryskin, 1978). Atomic motions along the symmetry axis (sometimes referred to as the "A-species") are unique from those that are perpendicular with respect to the axis ("E-species"). The A-species include the stretch and translation vibrations. The anti-symmetric E-species include librations (rocking) and one translation. Vibrations of the same species can couple and mix. These six vibrations produce four distinct frequencies.

The OH groups of the brucite unit cell are related through a center of symmetry so that they produce four IR active modes that are anti-symmetric with respect to the center of symmetry (there are also four Raman active modes). The modes symmetric with the center are IR inactive. When the Mg^{2+} ion is included in the analysis, it can only participate in the IR active OH modes. In the OH-stretching region this is observed as the single absorption band at 3698 cm^{-1} (Fig. 7). IR active Mg-O-H libration (bending) mode in brucite occurs at a lower frequency of 445 cm^{-1}. The bands at 571 cm^{-1} and 645 cm^{-1} also presumably involve Mg-O-H vibrations that similarly occur in the spectra of trioctahedral clays, such as talc and saponite.

Gibbsite, in contrast to brucite, contains Al^{3+} ions (each with six nearest oxygen neighbors). Gibbsite has an octahedral-edge sharing arrangement where two of three octahedral sites are occupied. This dioctahedral arrangement distorts the ideal octahdera and lowers the symmetry content of the unit cell

(Table 1). The higher electronegativity of the Al^{3+} ion enables the formation of moderately strong hydrogen bonds in OH^- groups.

For gibbsite, there are six four-fold sets of anions and six sets of hydrogen bonds. Stretching modes are observed in the room-temperature absorption spectrum (Fig. 8) where four modes are found over the range of 3617 to 3380 cm^{-1}. Studies at lower temperatures of oriented gibbsite crystals using polarized IR radiation (Russell et al., 1974) assigned the various bands to the six sets of OH groups. Four bands at 914, 972,1021 and 1060 cm^{-1} correspond to OH-bending vibrations that consist of the six independent sets of hydroxyls. Presumably the lower frequency band at 914 cm^{-1} is attributed to the Al-O-H group with the least hydrogen bonding influence. The bands in the 500 to 650 region are overlaps of out-of-plane OH bending vibrations and Al-O vibrations (Takamura and Koezuka, 1965).

Table 1. A comparison of the crystal-structure properties of brucite and gibbsite based on diffraction

Mineral formula	Space group	Formula per unit cell	Site symmetry and anion multiplicity	Octahedral site occupancy	M - OH distances (Å)	OH - OH distances (Å)
* $Mg(OH)_2$	D^3_{3d}	$Z = 1$	C_{3v} (2)	3	2.102	3.218
# $Al(OH)_3$	C^5_{2h}	$Z = 8$	$6C_1$ (4)	2	1.73 - 2.06	2.75, 2.80, 2.82, 2.94, 2.98, 3.10

* Zigan and Rothbauer (1967). # Megaw (1934); Bernal

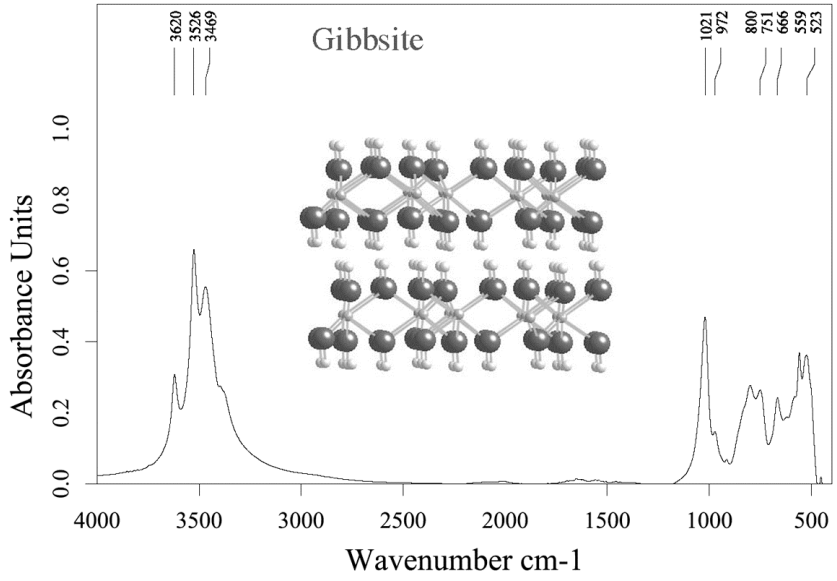

Figure 8. IR spectrum of gibbsite, $Al(OH)_3$, using 0.33 mg sample/ 150 mg KBr. Sample from Richmond, MA (Courtesy, James J. Howard). Crystal structural data from: Megaw (1934).

IR spectra of layer silicates

The primary basis for distinguishing phyllosilicates is the stacking arrangement of their planar sheets involving both Si-rich tetrahedral polyhedra and metal-rich octahedral polyhedra. Tetrahedral (**T**) and octahedral (**O**) sheets are bonded together as layer structures by either van der Waals forces, interlayer cations, or oxy-hydroxide interlayer cation sheets. A secondary distinction is made based on the dioctahedral (gibbsite-like) versus trioctahedral (brucite-like) nature of the octahedral sheets. Classification of the phyllosilicates is therefore broadly arranged into the 1:1 layer silicates (i.e., **T-O**), and 2:1 layer silicates (i.e., **T-O-T**). The magnitude of layer charge and the types of cations occupying inter- and intralayer sites further determine the basis for specific mineral group classification.

Farmer (1974) noted that vibrational modes of layer silicates are separated into constituent units that include (1) the hydroxyl groups, (2) silicate/aluminate groups with tetrahedral polyhedra, (3) octahedral metal cations, and (4) interlayer cations and molecules. The OH stretching modes common in most layer silicates lie in the 3400 to 3750 cm^{-1} region. OH bending (librations) modes occur in the 600 to 950 cm^{-1} region. Si-O and Al-O stretching modes associated with tetrahedral polyhedra are found in the 700 to 1200 cm^{-1} range and they only weakly couple with other vibrations in the structure. Si-O and Al-O bending modes associated with tetrahedral polyhedra dominate the 150 to 600 cm^{-1} region and are sometimes strongly coupled with the octahedral cations and translational modes of the hydroxyl groups (Farmer, 1974).

Vibrational modes of the interlayer cation are typically very low in frequency and occur in the far-IR region (50 to 150 cm^{-1}). As noted above, the focus of this chapter is on the mid-IR spectral response of phyllosilicates, therefore far-IR spectra are not presented here. However, far-IR spectroscopy offers great potential to characterize the interlayer environment of clay minerals, where cations can be used to probe the properties of exchangeable sites. See Prost and Laperche (1990), Laperche and Prost (1991) and Schroeder (1990; 1992) for more details on far-IR spectroscopy of clay minerals.

1:1 layer silicates

The kaolin and serpentine-group minerals represent the dioctahedral and trioctahedral 1:1 layer silicates respectively. A comparison of the IR spectra of kaolinite and lizardite shows the important structural effects of dioctahedral versus trioctahedral site occupancy on the orientation of hydroxyl groups. The IR spectra of kaolinite have been most extensively studied of all clay minerals. In particular, the interpretation of the OH stretching region has received special scrutiny (Farmer, 2000; Frost et al., 1998; Bish and Johnston, 1993). Figure 9 shows the typical absorption spectra for kaolinite powder.

The octahedral sheet of kaolinite is dominated by Al^{3+} cations with two out of every three octahedral sites occupied. The effect of the site vacancy is a lattice distortion and lowering of the crystal site symmetry (see discussion above re:

gibbsite versus brucite). The inner-surface hydroxyl groups therefore occur with slightly different orientations. The result is three unique inner-surface stretching modes that are observed at 3694, 3668, and 3652 cm^{-1} (Fig. 9). The orientation of the hydroxyl groups can not be determined from these random powder spectra. However, by combining polarized and single-crystal IR spectroscopy and using hydrazine intercalation (i.e., intercalation of organic molecules between layers) it has been shown that these inter-surface modes lie more perpendicular, than parallel to the layers (Frost et al., 1998). This near-perpendicular arrangement allows for the protons to optimally interact with the basal oxygen of the adjacent silicate tetrahedral sheet.

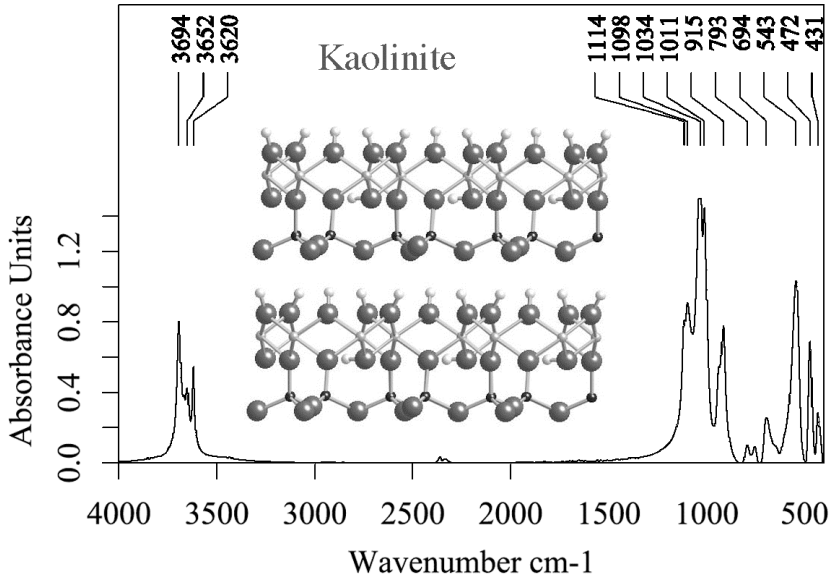

Figure 9. IR spectrum of kaolinite, $Al_2Si_2O_5(OH)_4$, using 0.33 mg sample/150 mg KBr. Sample from Buffalo Creek, Mine, Deep Step, GA. Crystal structural data from Bish (1993)

The band at 3620 cm^{-1} for kaolinite is a consequence of an inner hydroxyl stretch with its vector orientation near to the (001) plane (pointed in the direction of the vacant octahedral site; see Fig. 1). This inner hydroxyl group results from bonding between a proton and an oxygen that is also coordinated to Al^{3+} in an octahedral site. The proton lies in a plane close to the apical oxygen of the tetrahedral sheet. In-plane bending vibrations of the surface hydroxyl groups in kaolinite occur at 937 cm^{-1}, whereas the inner hydroxyl bending vibration occurs at 915 cm^{-1}.

The hydroxyl-stretch region for lizardite, shown in Figure 10 reveals a less complex spectrum, where it appears that all the inner-layer hydroxyl stretching modes occur near the frequency of 3686 cm^{-1}. It is not possible to

distinguish between the inner-layer hydroxyl groups from the outer-layer hydroxyl groups. The trioctahedral structure of lizardite has greater symmetry than kaolinite. Higher symmetry of the sites promotes degeneracy of optic modes and powder preparations can not make hydroxyl group distinctions. This result is supported by the strong absorption of the bending vibrations of the hydroxyl groups in the octahedral sheet of lizardite. Note that the modes at 600 to 660 cm^{-1} are considerably higher than the brucite modes (~450 cm^{-1}) and, as shown below, lower than their counterpart 2:1 layer in talc at 670 cm^{-1}.

In both kaolinite and lizardite, the presence of bands in the 1100 to 1000 cm^{-1} region is related to Si-O stretching modes. Stresses imparted by distortions of the octahedral sheet in kaolinite are transfer to the tetrahedral sheet. This distortion of the tetrahedral sheet in kaolinite reduces the degeneracy of the Si-O modes. This degeneracy is observed by comparing the kaolinite and lizardite spectra and noting the additional bands found in the kaolinite lattice-stretch region.

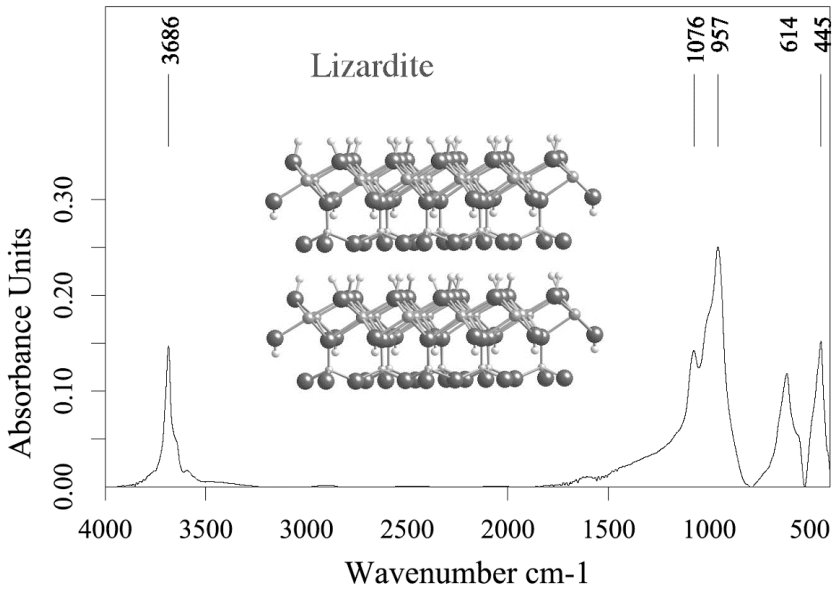

Figure 10. IR spectrum of lizardite, $Mg_3Si_2O_5(OH)_4$, using 0.38 mg sample/150 mg KBr. Sample from Coulterville CA. Crystal structural data from Mellini and Zanazzi (1987).

For all powder samples prepared at room temperature, low intensity broad absorption bands often occur in the spectra owing to adsorbed molecular H_2O. This is observed in most spectra by the occurrence of low frequency shoulders (~3400 cm^{-1}) on the bands in the hydroxyl stretching region and by a low intensity, broad band near 1640 cm^{-1}. These bands sometimes do not occur if the samples are heated to 150° C. However, as noted above, reactions may

occur between some clays (e.g., halloysite and smectites) and the KBr. This might modify other portions of the spectrum (see appendix).

2:1 layer silicates with zero layer charge

Talc (trioctahedral) and pyrophyllite (dioctahedral) are end-member examples of the basic 2:1 structure, from which the nature of true micas, brittle micas and other 2:1 clay minerals can be derived. The 1:1 layers differ from 2:1 layers by the addition of a tetrahedral sheet and a replacement of surface-hydroxyl groups of the 1:1 layers by a second inverted silicate tetrahedral sheet (Fig. 11). Thus, the inner-hydroxyl groups of the octahedral sheet remains.

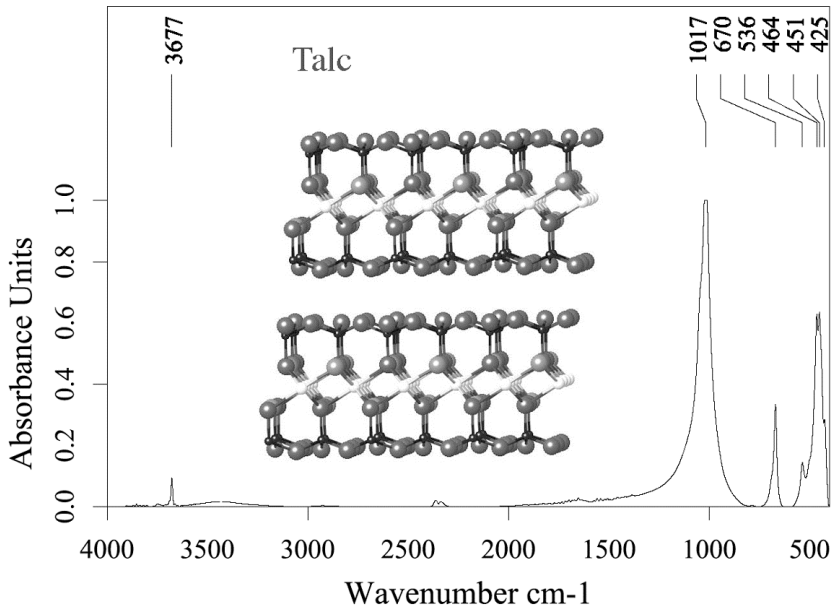

Figure 11. IR spectrum of Talc, $Mg_3AlSi_3O_{10}(OH)_2$, using 0.37 mg sample/ 150 mg KBr. Sample from Hartford County, PA (Courtesy Yale Peabody Museum B-4761). Crystal structural data from Rayner and Brown (1973). Protons not shown.

The OH-stretching frequency of the octahedral Mg-O-H unit in talc occurs at 3677 cm^{-1}. The high site symmetries of the trioctahedral talc structure results in the degeneracy of the OH sites, and therefore only one band is observed in a spectrum from a powder. If Mg^{2+} is replaced by a higher-mass divalent cation (e.g., Ni^{2+}) then four possible sites are found (Wilkins and Ito, 1967). Note that the Mg^{2+} ionic radius is smaller (0.65Å) than that of Ni^{2+} (0.72 Å). The greater size and mass of each Ni atom is observed as bands with lower frequencies. The resultant sites are made from the destruction of translational symmetry in the lattice. The libration modes of the Mg-O-H in end-member talc are observed in bands at 670 cm^{-1} and 464 cm^{-1}, respectively.

The lattice vibrations of talc are described by a pseudo-hexagonal silicon and oxygen-rich sheet with a near six-fold symmetry axis and seven atoms in the unit cell (Ishii et al., 1967). The possible IR active vibrational modes of the idealized tetrahedral sheet are classified into five groups of modes. Two are singly degenerate symmetric stretches at 902 and 611 cm^{-1} and three are doubly degenerate modes at 1017, 543, and 285 cm^{-1} (Fig. 11). For the purposes of this chapter only the 400 to 4000 cm^{-1} region is being considered and the lowest frequency mode at 285 cm^{-1} is not shown. However, if appropriately different beam splitter and detector configurations are used, then this mode can be examined. Such systems are not routinely found in introductory chemistry teaching laboratories.

The mid-IR absorption spectrum of pyrophyllite is more complex relative to talc (i.e., more absorption bands occur) owing to the site symmetry reduction resulting from vacant octahedral sites. The misfit between the octahedral and tetrahedral sheets is partially accommodated by a half clockwise and half counter-clockwise rotation of the pseudo-hexagonal network. Distortion to the tetrahedral ring within the sheet also occurs by individual tilting of the silicate tetrahedra. The symmetry reduction caused by tetrahedral rotation alone increases the number of IR active modes from five to nine for the silicate layer (Ishii et al., 1967).

Despite the reduction of site symmetry in pyrophyllite relative to talc, some absorption features observed in talc also occur in the spectra of pyrophyllite and other dioctahedral 2:1 silicates. For pyrophyllite, the Si-O vibration occurs in the 1067 cm^{-1} region (Fig. 12). Several additional bands appear in the 950 to 1100 cm^{-1} range for pyrophyllite. The degenerate modes of the Si-O stretching vibrations that were present in talc are no longer present in

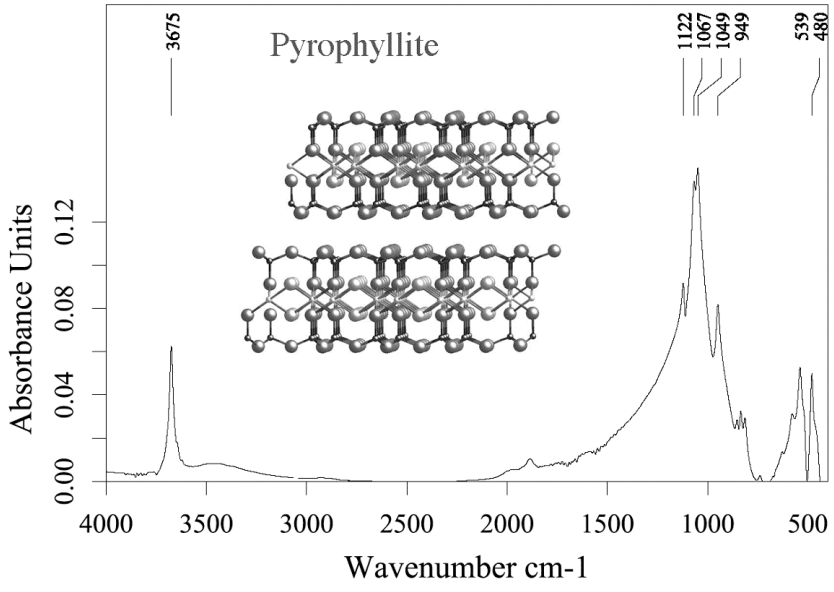

Figure 12. IR spectrum of pyrophyllite, $Al_2AlSi_3O_{10}(OH)_2$, using 0.39 mg sample/ 150 mg KBr. Sample from Robbins, NC. Crystal structural data from Lee and Guggenheim (1981). Protons not shown.

pyrophyllite. Si-O bending modes in pyrophyllite also appear to contribute significantly to absorption in the 450 to 550 cm^{-1} range. In contrast to talc, the greater distortion of the dioctahedral structure causes the frequencies of the bands to be sensitive to ionic substitution.

As a general rule, the wavenumber varies inversely with the ionic radius of the dioctahedral cation (Stubican and Roy, 1961). For example, the substitution of Fe^{3+} for Al^{3+} (ionic radii of 0.64 Å and 0.50 Å, respectively) produces a lower frequency band. IR spectroscopy therefore, serves as a useful tool to compare closely related clay mineral species with small differences in dioctahedral site occupancy (e.g., Vantelon et al., 2001).

2:1 layer silicates with layer charge

Negative layer charge most commonly develops in 2:1 structures because of ionic substitution (e.g., Al^{3+} for Si^{4+} in the tetrahedral sheet or Mg^{2+} for Al^{3+} in the octahedral sheet). The net magnitude of 2:1 layer charge (x) can range anywhere from < 0 to -2 per half unit cell. The number of possible interlayer cations, interlayer sheets, and interlayer molecules that compensate for charge imbalance is large. Consequently 2:1 layer silicates vary greatly in composition. Martin et al. (1991) discussed 2:1 classification and grouped those minerals with a 2:1 layer in the following manner: (1) the brittle micas ($x \sim 1.8 – 2.0$; e.g., margarite), (2) true micas ($x \sim 0.6 – 1.0$, with non-hydrous interlayer cations; e.g., muscovite, biotite, phlogopite, and illite,), (3) chlorites ($x \sim 0.6 – 1.0$, with brucite-like and gibbsite-like interlayer sheets; e.g., clinochlore and chamosite), (4) vermiculites ($x \sim 0.6 – 0.9$ with hydrous interlayer cations; e.g., vermiculite), (5) smectites ($x \sim 0.0 – 0.6$ with hydrous interlayer cations; e.g., montmorillonite and saponite), (6) modulated structures (e.g., sepiolite and palygorskite), (7) regularly interstratified clays (e.g., rectorite, corrensite, hydrobiotite), and (8) randomly interstratified clays composed of any combination of 2-5 and 7 above (e.g., biotite-vermiculite and illite-montmorillonite). The assignment of bands observed in the spectra of many clay minerals, as a function of their various states of interlayer hydration and intralayer site ordering is still very much a part of active research. To consider the IR spectral properties of all these minerals is beyond the scope of this chapter.

For illustrative purposes, the IR spectrum for a representative chlorite structure, clinochlore, is given in Figure 13. Clinochlore represents just one of several known chlorite-group minerals, in which octahedral sheets occupy the 2:1 interlayer positions. Specifically in clinochlore, Al^{3+} substitution for Si^{4+} in the tetrahedral sheet imparts a net negative layer charge for the tetrahedral sheet. Substitution of Al^{3+} for Mg^{2+} in a brucite-like sheet creates a net positively charged interlayer that compensates and neutralizes the overall structure.

If Al^{3+} substitution occurs in a regularly patterned order within the tetrahedral sheet, then a larger unit cell must be employed to include the

symmetry of the lattice. The effect of Al^{3+} substitution for Si^{4+} into a pseudo-hexagonal tetrahedral sheet (without distortion) even further reduces symmetry. Assuming the Al is evenly distributed, then 39 IR active modes are expected (Ishii et. al., 1967). With so many additional IR active modes, a broadening of the absorption bands is expected.

Comparing the spectra of clinochlore with talc (Figs. 11 and 13) does show a general broadening of all bands in clinochlore relative to talc. The presence of two additional bands (3575 and 3428 cm^{-1}) associated with the interlayer hydroxyl sheet of clinochlore also provides clear evidence for O-H stretches in the interlayer sheet and molecular H_2O. Note that the interlayer hydroxyl groups have lower frequency modes (i.e., longer O-H distances) than the inner hydroxyl groups at 3698 cm^{-1} and 3676 cm^{-1} common to both talc and clinochlore, respectively. The bending vibrations of Mg-O-H groups in the 600 to 670 cm^{-1} range are seen in clinochlore and talc, as well as lizardite (see Fig. 10; and Farmer, 1974). The higher frequency bending vibrations of Al-O-H groups in the 700 to 800 cm^{-1} region are seen in spectra of clinochlore and absent in spectra of talc.

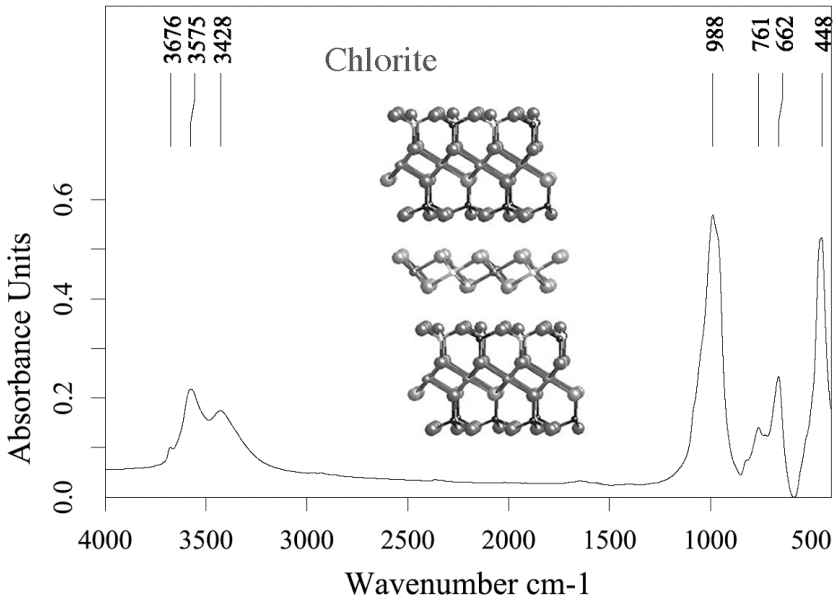

Figure 13. IR spectrum of clinochlore, $Mg_3AlSi_3O_{10}(OH)_2$ $Mg_3Al(OH)_6$, using 0.39 mg sample/150 mg KBr. Sample from Westchester, PA (Courtesy Yale Peabody Museum PM-5247). Crystal structural data from Phillips et al. (1980). Protons not shown.

For 2:1 structures, misfit between the octahedral sheet and tetrahedral sheets, results in tetrahedral rotation (Bailey, 1984). Tetrahedral rotation increases with increasing dioctahedral nature relative to trioctahedral sheets. Rotation also generally increases with increasing tetrahedral Al^{3+}, as

exemplified in the extreme case of the brittle micas (Guggenheim, 1984). The implication for increased tetrahedral rotation is a decrease in site symmetry. This is manifested in IR spectra as a broadening and shifting of Si-O stretching modes in the 900 to 1100 cm^{-1} region. In talc, the isolated band at 1017 cm^{-1} is from Si_4O_{10} and this band is sharper and higher in frequency than the 988 cm^{-1} band that results from $AlSi_3O_{10}$ portion of clinochlore.

SUMMARY

The collection and analysis of IR spectral data is a simple way to gain insight into the octahedral, tetrahedral and hydroxyl structural units of clay minerals. The student will be challenged in that not all band assignments are known for clay minerals. Students should be encouraged to explore IR spectroscopy as a valuable empirical tool with the potential for quantification of certain adsorbed and structural species.

Mid-IR data collection using FTIR spectrometers is rapid, and sample preparation methods are straightforward. The spectra of well–ordered, end-member hydroxides, 1:1, and 2:1 layer silicates (e.g., brucite, gibbsite, kaolinite, talc, and pyrophyllite) can be examined first to establish the nature of band assignments and the relationship between crystal symmetry and band positions. Subsequent comparison of clay minerals with well–ordered stacking and poorly-ordered stacking allows empirical predictions about differences in the crystal chemistry of clays. Coupled ionic substitutions and differences in the orientation of hydroxyl groups are, in part, responsible for variations in IR spectral responses. The expanded phase activities that follow can for example, show how the IR spectra of smectite respond to changes in hydration state and the type of exchangeable interlayer cation.

Modern IR techniques that allow measurement of (1) reflectance properties, (2) responses to environmental conditions (e.g., heating and cooling stages), and (3) the near-IR and far-IR region are becoming more widely available for teaching and demonstration purposes. As band assignments and our understanding of spectral response to changes in clay crystal chemistry (i.e., variations in both interlayer and intralayer cation compositions and hydration states) are more fully developed, IR spectroscopy will become an even more powerful tool for teaching clay science. However, no technique stands alone and all applicable forms of spectroscopy, diffraction, and crystal chemistry should be employed to develop a more accurate picture of clay mineral crystal chemistry.

ACKNOWLEDGEMENTS

The editorial comments of the workshop organizers, Stephen Guggenheim and Audrey Rule, are greatly appreciated. Colin Farmer's review comments clarified much of the band-assignment discussion. Jana Madejova and Peter Komadel also improved the manuscript. The spectrometer used to collect the IR data was made possible by a grant to the author from the National Science Foundation Instrument Facilities Program (EAR-9911501).

REFERENCES CITED

Bailey, S.W. (1984) Crystal Chemistry of the true micas. In Reviews in Mineralogy: Micas, (Ed) S.W. Bailey. Mineralogical Society of America, Washington, D.C. **13**, 13-60.

Bernal, J.D. and H.D. Megaw (1935) The function of hydrogen in intermolecular forces. Proceedings of the Royal Society, **151A,** 384-420.

Bish, D. L. (1993) Rietveld refinement of the kaolinite structure at 1.5K. Clays and Clay Minerals, **41**, 738-344.

Bish, D.L. and C.T. Johnston (1993) Rietveld refinement and Fourier-transform infrared spectroscopic study of the dickite structure at low-temperature. Clays and Clay Minerals, **41,** 297-304.

Calas, G. and F.C. Hawthorne (1988) Introduction to spectroscopic methods. In Reviews in Mineralogy: Spectroscopic methods in mineralogy and geology, (Ed) F.C. Hawthorne. Mineralogical Society of America, Washington, D.C. **18**, 1-10.

Farmer, V.C. (2000) Transverse and longitudinal crystal modes associated with OH stretching vibrations in single crystals of kaolinite and dickite Spectrochimica Acta **56** 927-930.

Farmer, V.C. (1974) The layered silicates In: The infrared spectra of minerals (Ed.) V.C. Farmer. The Mineralogical Society Monograph 4. London. 331-363.

Frost R.L., J. Kristof, G.N. Paroz, T.H. Tran, and J.T. Kloprogge (1998) The role of water in the intercalation of kaolinite with potassium acetate. Journal of colloid and interface science, **204**, 227-236.

Guggenheim, S. (1984) The brittle micas. In Reviews in Mineralogy: Micas, (Ed) S.W. Bailey. Mineralogical Society of America, Washington, D.C. **13**, 61-104.

Harris, D.C. and M.D. Bertolucci (1978) Symmetry and spectroscopy: An introduction to vibrational and electronic spectroscopy. Dove Publications, Inc. New York. 550 pp.

Ishii, M., T. Shimanouchi and M. Nakahira (1967) Far infrared absorption spectra of layered silicates. Inorganica Chimica Acta, **1**, 387-392.

Kubicki, J.D. 2001 Interpretation of vibrational spectra using molecular orbital theory calculation. In Reviews in Mineralogy: Molecular modeling theory: Applications in the geosciences, (Eds.) R.T. Cygan and J.D. Kubicki. Mineralogical Society of America, Washington, D.C. **42**, 459-484.

Lee, J.H. and S. Guggenheim (1981) Single-crystal X-ray refinement of pyophyllite-1TC. American Mineralogists, **66,** 350-357.

Laperche, V. and R. Prost (1991) Assignment of the far-infrared absorption bands of K in micas. Clays and Clay Minerals, **39,** 281-289.

Madajová J. and P. Komadel (2001) Baseline studies of The Clay Minerals Society Source Clays: Infrared methods. Clays and Clay Minerals. **49,** 401-432.

Martin, R.T., S.W. Bailey, D.D. Eberl, D.S. Fanning, S. Guggenheim, H. Kodama, D.R. Pevear, J. Sorodon, and F.J. Wicks. (1991) Report of The Clay Minerals Society Nomenclature Committee: Revised classification of clay minerals. Clays and Clay Minerals, **39,** 329-332.

McMillan, P.F. and A.C. Hess (1988) Infrared and Raman spectroscopy. In Reviews in Mineralogy: Spectroscopic methods in mineralogy and geology, (Ed.) F.C. Hawthorne. Mineralogical Society of America, Washington, D.C. **18**, 99-159.

Megaw H. (1934) The crystal structure of hydroargillite, $Al(OH)_3$ Zietschift Kristallograhie und Mineralgie 185-204.

Mellini, M., and P.F. Zanazzi, (1987) Crystal structures of lizardite-1T and lizardite-$2H_1$ from Coli, Italy. American Mineralogist, **72**, 943–948.

Palmer, D. (2001) CrystalMaker. A computer program for plotting crystal structures. v. 5.0.3 CrystalMaker Software, Bichester, Oxfordshire, UK.

Pelletier M, L.J. Michot, O. Barres, B. Humbert, S. Petit, J.-L. Robert (1999) Influence of KBr conditioning on the infrared hydroxyl-stretching region of saponites. Clay Minerals. **34** 439-445.

Phillips. T.L., J.K. Loveless, and S. W. Bailey. (1980) Cr^{3+} coordination in chlorites – Structural study of 10 chromian chlorites. American Mineralogist **65**, 112-122

Prost R. and V. Laperche (1990) Far-infrared study of potassium micas. Clays and Clay Minerals, **38,** 351-355.

Rayner, J.H. and G. Brown (1973) The crystal structure of talc. Clays and Clay Minerals, **21,** 103-114.

Russel, J.D. and A.R. Fraser (1994) Infrared Methods In: Clay Mineralogy: Spectroscopic and Chemical Determinative methods. (Ed.) M.J. Wilson. Chapman and Hall, London. 11- 67.

Russel, J.D., R.L. Parfitt, A.R. Fraser, V.C. Farmer (1974) Surface structures of gibbsite, goethite and phosphated goethite. Nature, **248**, 220-221.

Ryskin, Y.A. (1974) The vibrations of protons in minerals: hydroxyl, water and ammonium. In: The infrared spectra of minerals (Ed.) V.C. Farmer. The Mineralogical Society Monograph 4. London. 137-181.

Schroeder, P.A. (1992) Far infrared study of the interlayer torsional-vibrational mode of mixed-layer Illite-smectites. Clays and Clay Minerals, **40**, 81-91.

Schroeder, P.A. (1990) Far infrared, X-ray diffraction and chemical investigation of potassium micas: American Mineralogist, **75**, 983-991.

Schroeder, P.A., and E.D. Ingall (1994) A method for the determination of nitrogen in clays, with application to the burial diagenesis of shales. Journal Sedimentary Research, **A64**, 694-697.

Stubican, V. and R. Roy. (1961) isomorphous substitution and infrared spectra of layer lattice silicates. American Mineralogist, **46**, 32-51.

Takamura, T. and J. Koezuka (1965) Infrared evidence of grinding effect on the hydrargillite single crystals. Nature, **207,** 965.

Vantelon, D., M. Pelletier, L. J. Michot, O. Barres, and F. Thomas (2001) Fe, Mg and Al distribution in the octahedral sheet of montmorillonites. An infrared study in the OH-bending region**.** Clay Minerals. **36,** 369-379.

Wilkins, R.W.T. and J. Ito (1967) Infrared spectra of some synthetic talcs. American Mineralogist, **52**, 1649-1661.

Zigan, F. and R. Rothbauer. (1967) Neutron diffraction measurements of brucite Neues Jahrbuch fuer Mineralogie. Monatshefte. **4-5**, 137-143.

LABORATORY EXERCISE IN INFRARED SPECTROSCOPY

Required materials

Smectite – e.g., The Clay Minerals Society Source Clay STx-l, NH_4Cl, $MgCl_2$, KBr (IR-grade), 13 mm pellet die, deionized water, 150 ml beaker, Centrifuge (optional), FTIR spectrometer, Oven for heating to 180° C

The purpose of this laboratory exercise is to observe the effect of water and cation adsorption on smectite. We will exchange NH_4^+ and Mg^{2+} into the interlayer sites of the clay. Two KBr pellets will be prepared. Spectra will be collected at room temperature and then after heating to 180° C.

Procedures

1. Weigh two 0.5 g aliquots of smectite and place each into separate 150 ml beakers.
2. Add 5 grams of NH_4Cl and 100 ml of water to one beaker. Add 1 gram of $MgCl_2$ and 100 ml of water to the other beaker. These solutions will make approximately 1 and 0.1 molar solutions of NH_4^+ and Mg^{2+}, respectively. Stir each for 30 seconds and let stand until the clay has settled (about 10 minutes).
3. Remove the excess salt ions by washing with deionized water. This is done by slowly decanting the fluid above the clay VERY carefully, so as not to lose clay.
4. Add 100 ml of deionized water to the beakers and continue to decant each beaker after the clay has settled. You might note that each time it takes longer for the clay particles to settle. If you have access to a centrifuge, then you can speed this process by settling the clay in centrifuge tubes and by pouring off the clear fluid above the clay. Three rinse cycles should be sufficient to remove excess cations and Cl^-.
5. Remove excess water from the clays by either drying on filter paper or by drying overnight in a watch glass at room temperature.
6. Prepare a pressed pellet for each cation-saturated clay using 1.0 mg of clay with 200 mg of KBr. You may want to prepare extra in case of breakage later.
7. Collect IR spectra for each pellet at room temperature.
8. Heat each pellet to 180° C for 2 hours and then collect IR spectra.
9. Plot each spectrum over the range of 3800 to 1300 cm^{-1}.

Analysis and discussion after completing the experiments

1. Estimate a baseline for the Mg^{2+} and NH_4^+-saturated smectite spectra. Do this by either using software resident on the spectrometer computer or by sketching a smooth baseline on a paper print out.

2. Estimate the intensity (baseline to peak) in absolute units of absorbance at the following frequencies: 3625 cm^{-1}, 3442 cm^{-1}, 3187 cm^{-1}, 1635 cm^{-1} and 1405 cm^{-1}.
3. Assign these bands to a structural component of the smectite.

Questions for discussion

Can you identify evidence for free molecular H_2O and structural hydroxyl groups in the spectra? Is the frequency of free molecular H_2O different from molecular H_2O coordinated to an interlayer cation?

Is there evidence for molecular H_2O being present in the heated samples? Why would Mg^{2+} retain H_2O, but NH_4^+ not retain H_2O after heating?

Can you find evidence for NH_4^+ adsorption in the spectra? Why is the frequency of adsorbed NH_4^+ at 1402 cm^{-1} different from the frequency of fixed NH_4^+ at 1435 cm^{-1}?